

# SCIENTIFIC REPORTS



OPEN

## Unique Roles of $\beta$ -Arrestin in GPCR Trafficking Revealed by Photoinducible Dimerizers

Osamu Takenouchi, Hideaki Yoshimura &amp; Takeaki Ozawa

Intracellular trafficking of G protein-coupled receptors (GPCRs) controls their localization and degradation, which affects a cell's ability to adapt to extracellular stimuli. Although the perturbation of trafficking induces important diseases, these trafficking mechanisms are poorly understood. Herein, we demonstrate an optogenetic method using an optical dimerizer, cryptochrome (CRY) and its partner protein (CIB), to analyze the trafficking mechanisms of GPCRs and their regulatory proteins. Temporally controlling the interaction between  $\beta$ -arrestin and  $\beta$ 2-adrenergic receptor (ADRB2) reveals that the duration of the  $\beta$ -arrestin-ADRB2 interaction determines the trafficking pathway of ADRB2. Remarkably, the phosphorylation of ADRB2 by G protein-coupled receptor kinases is unnecessary to trigger clathrin-mediated endocytosis, and  $\beta$ -arrestin interacting with unphosphorylated ADRB2 fails to activate mitogen-activated protein kinase (MAPK) signaling, in contrast to the ADRB2 agonist isoproterenol. Temporal control of  $\beta$ -arrestin-GPCR interactions will enable the investigation of the unique roles of  $\beta$ -arrestin and the mechanism by which it regulates  $\beta$ -arrestin-specific trafficking pathways of different GPCRs.

The localization and degradation of membrane proteins are regulated by intracellular trafficking<sup>1,2</sup>. The precise regulation of membrane proteins stimulated by membrane receptors is important for cells to adapt to a wide variety of extracellular stimuli. The perturbation of trafficking systems induces important diseases, including diabetes, cancers and neurodegenerative diseases<sup>3-6</sup>. Investigating the trafficking mechanism is therefore important for drug development and therapeutics. Intracellular trafficking is regulated by many proteins.  $\beta$ -Arrestin is a representative of these proteins and regulates the localization of membrane receptors, such as G protein-coupled receptors (GPCRs)<sup>7,8</sup>, growth factor receptors (transforming growth factor receptor (TGFR) and insulin-like growth factor receptor (IGFR))<sup>9,10</sup>.  $\beta$ -Arrestin is recruited to ligand-bound GPCRs and sequesters the receptor from the cell surface by endocytosis. Imaging of GPCRs and  $\beta$ -arrestin revealed that GPCRs that stably interact with  $\beta$ -arrestin are retained in the cytosolic compartment, whereas GPCRs that immediately dissociate from  $\beta$ -arrestin are rapidly recycled back to the cell membrane<sup>11-13</sup>. These results suggest a significant role for  $\beta$ -arrestin in the intracellular trafficking of GPCRs. In addition, GPCR-bound  $\beta$ -arrestin functions as a signal transducer of mitogen-activated protein kinases (MAPKs) and the Ser-Thr kinase Akt in the trafficking pathway<sup>14</sup>. Despite the significance of  $\beta$ -arrestin-related trafficking, the manner by which  $\beta$ -arrestin switches the trafficking pathways of GPCRs in living cells is unclear.

Optogenetics, in combination with fluorescence and bioluminescence imaging techniques, is a useful technique for the spatiotemporal analysis of intracellular signaling. Photodimerizing proteins, one of many photoreceptor derived tools, are often used to control the interactions of specific proteins in living cells<sup>15-17</sup>. When the cryptochrome (CRY) derived from *Arabidopsis thaliana* absorbs blue light, it interacts with cryptochrome-interacting basic-helix-loop-helix 1 (CIB)<sup>18,19</sup>. An attractive feature of this system is that CRY and CIB reversibly interact and rapidly associate and dissociate. Herein, we demonstrate an optogenetic approach using the reversible interaction between CRY and CIB to investigate the significance of the interaction of  $\beta$ -arrestin with GPCRs in intracellular trafficking in living cells. Our method reveals that the light-induced interaction of  $\beta$ -arrestin with the  $\beta$ 2-adrenergic receptor (ADRB2) is sufficient to trigger endocytosis of ADRB2 without ADRB2 being phosphorylated. We also clarify that the dissociation of  $\beta$ -arrestin promotes the recycling of ADRB2 to the plasma membrane, whereas prolonged interaction of  $\beta$ -arrestin with ADRB2 directs ADRB2 to

Department of Chemistry, Graduate School of Science, The University of Tokyo, 7-3-1 Hongo, Bunkyo-ku, Tokyo, 113-0033, Japan. Correspondence and requests for materials should be addressed to T.O. (email: [ozawa@chem.s.u-tokyo.ac.jp](mailto:ozawa@chem.s.u-tokyo.ac.jp))

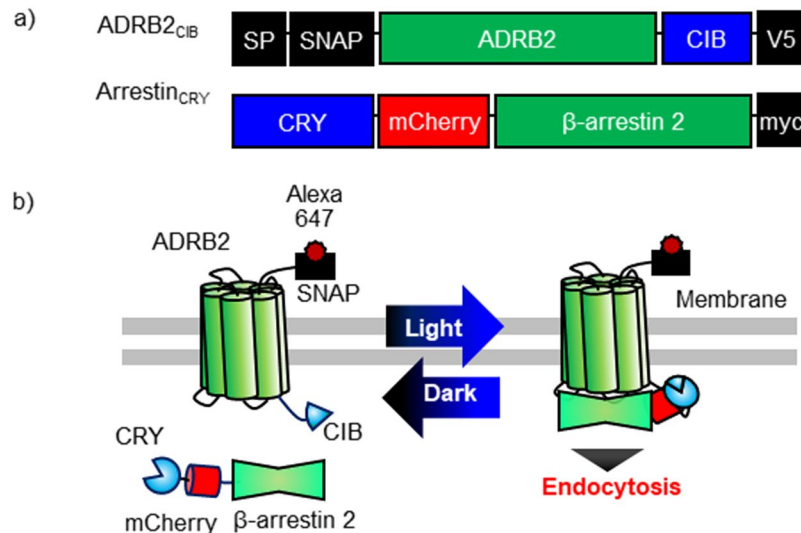


**Figure 1.** Light-based manipulation of reversible interaction between  $\beta$ -arrestin and ADRB2 using photodimerizers. **(a)** Schematic structures of the optogenetic manipulation system for the reversible interaction of  $\beta$ -arrestin with ADRB2. ADRB2<sub>CIB</sub> is composed of a signal peptide (SP) derived from 5HT3A serotonin receptor that targets the protein to the cell membrane, a SNAP-tag, a  $\beta$ 2-adrenergic receptor (ADRB2), a CIB, and a V5 epitope tag. Arrestin<sub>CRY</sub> consists of a cryptochrome (CRY), an mCherry, a  $\beta$ -arrestin2, and a myc epitope tag. **(b)** Basic principle of light-induced interaction of  $\beta$ -arrestin2 with ADRB2. Before light stimulation, ADRB2<sub>CIB</sub> localizes on the cell membrane, and Arrestin<sub>CRY</sub> distributes throughout the cytosol. Upon stimulation with blue light, Arrestin<sub>CRY</sub> interacts with ADRB2<sub>CIB</sub>, which triggers the endocytosis of the ADRB2<sub>CIB</sub>-Arrestin<sub>CRY</sub> complex. Under dark conditions, Arrestin<sub>CRY</sub> dissociates from ADRB2<sub>CIB</sub> and redistributes into the cytosol.

the lysosomal pathway. These results demonstrate the significant role of the duration of the  $\beta$ -arrestin-ADRB2 interaction in sorting between intracellular trafficking pathways in living cells.

## Result

**Basic Strategy for Light-Induced Interactions between ADRB2 and  $\beta$ -Arrestin.** ADRB2 is a GPCR that regulates cardiovascular and pulmonary functions<sup>20,21</sup>. Isoproterenol chloride (ISO), a specific ligand of ADRB2, activates G protein-mediated signals and induces clathrin-mediated endocytosis of ADRB2 through its interaction with  $\beta$ -arrestin. To temporally control the interaction between ADRB2 and  $\beta$ -arrestin by external blue light, we connected SNAP-tag-fused ADRB2 to the N-terminus of CIB (named ADRB2<sub>CIB</sub>); in addition, mCherry-fused  $\beta$ -arrestin 2 was attached to the C-terminus of CRY (denoted Arrestin<sub>CRY</sub>) (Fig. 1a). Each domain was connected to flexible linkers composed of glycine and serine to allow the dynamic motion of the fusion proteins. Before blue light irradiation, ADRB2<sub>CIB</sub> locates on the cell membrane, and Arrestin<sub>CRY</sub> distributes throughout the cytosol (Fig. 1b). Stimulation with blue light induces translocation of Arrestin<sub>CRY</sub> to ADRB2<sub>CIB</sub> on the cell membrane by the interaction between CRY and CIB, thereby triggering endocytosis of ADRB2<sub>CIB</sub>-Arrestin<sub>CRY</sub> complexes. After irradiation is stopped, Arrestin<sub>CRY</sub> is redistributed in the cytosol by the dissociation of CRY and CIB.

**Light-Induced Endocytosis of ADRB2<sub>CIB</sub>.** To determine whether light irradiation controls the interaction between ADRB2 and  $\beta$ -arrestin, HEK293 cells stably expressing ADRB2<sub>CIB</sub> and Arrestin<sub>CRY</sub> (HEK293<sub>opt</sub>) were irradiated with blue light under a confocal fluorescence microscope (Fig. 2a, Movie S1). Arrestin<sub>CRY</sub> was translocated from the cytosol to the cell membrane a few min after the start of irradiation and then moved back into the cytosol to form a dot-like structure. ADRB2<sub>CIB</sub> fluorescent spots appeared in the cytosol at 15 min, and their number gradually increased until 30 min of irradiation. The fluorescent spots mostly colocalized with Arrestin<sub>CRY</sub>. In a control experiment, a fusion protein comprising SNAP-tag and ADRB2 without CIB was expressed in HEK293 cells. The localization of Arrestin<sub>CRY</sub> was unchanged upon stimulation with blue light due to the lack of the CIB portion (Supplementary Fig. 1a). Furthermore, fluorescent spots in the HEK293 cells expressing Arrestin<sub>CRY</sub> and cell membrane-anchored CIB (Myr-Venus-CIB) were not observed during irradiation, despite Arrestin<sub>CRY</sub> being translocated to the cell membrane. To analyze the results quantitatively, we counted the number of spots containing ADRB2<sub>CIB</sub>, ADRB2, and Myr-Venus-CIB in the obtained images (Supplementary Fig. 1b). A significant increase in the number of spots was observed after light irradiation in case of ADRB2<sub>CIB</sub>. In contrast, the number of spots containing ADRB2 or Myr-Venus-CIB did not change after light stimulation. The results indicate that recruitment of  $\beta$ -arrestin to ADRB2 is necessary for appearance of the spots. In addition, the cells expressing Myr-Venus-CIB and Arrestin<sub>CRY</sub> were irradiated for 120 min (Supplementary Fig. 1c). The number of spots containing Myr-Venus-CIB did not increase under the prolonged irradiation.

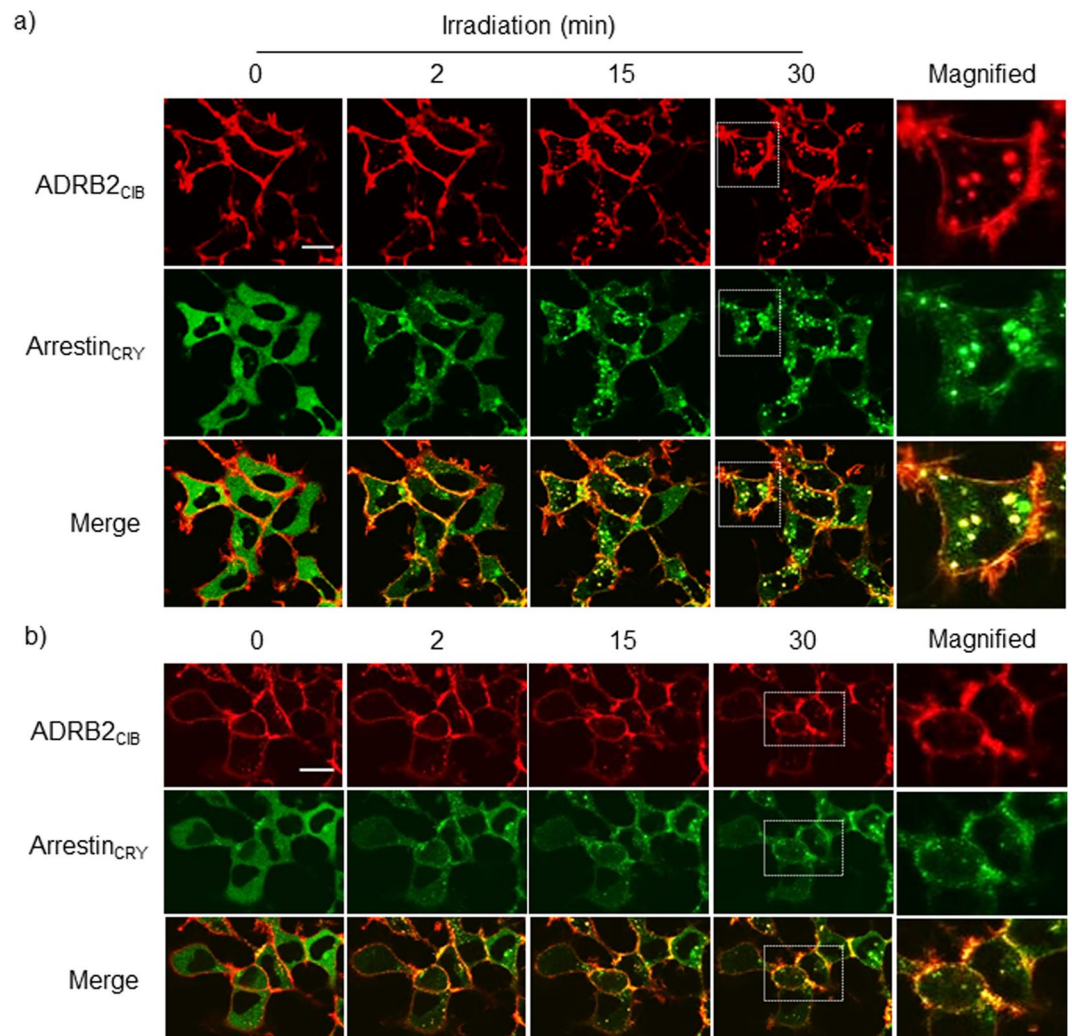


**Figure 2.** Light-induced endocytosis of ADRB2<sub>CIB</sub>. Images of ADRB2<sub>CIB</sub> and Arrestin<sub>CRY</sub> fluorescence in HEK293<sub>opt</sub> cells irradiated with blue light for 0, 2, 15 and 30 min under a confocal microscope (a), and images of these cells pretreated with 30  $\mu$ M Dyngo4a for 30 min and then irradiated by blue light for 0, 2, 15 and 30 min (b). Red, ADRB2<sub>CIB</sub>; green, Arrestin<sub>CRY</sub>. Scale bar, 20  $\mu$ m.

We next examined the endocytosis of ADRB2 after ADRB2<sub>CIB</sub>-Arrestin<sub>CRY</sub> interaction. ADRB2 is endocytosed with  $\beta$ -arrestin in a clathrin-mediated manner<sup>22</sup>. Segregation of clathrin-coated pits from the cell membrane is regulated by dynamin GTPases. To show that the fluorescent spots resulted from clathrin-mediated endocytosis, we pretreated the HEK293<sub>opt</sub> cells with a dynamin inhibitor, Dyngo4a. The fluorescent spots did not appear in the presence of Dyngo4a after the stimulation by light (Fig. 2b). To quantitate this inhibitory effect, we quantified the number of ADRB2<sub>CIB</sub> fluorescent spots and the colocalization of Arrestin<sub>CRY</sub> with ADRB2<sub>CIB</sub> using the quantitative parameter Manders' colocalization coefficient, which is proportional to the total amount of fluorescence intensity from Arrestin<sub>CRY</sub> in the pixels where it colocalizes with ADRB2<sub>CIB</sub> (Supplementary Fig. 2a,b). The number of spots increased with prolonged irradiation time in the absence of Dyngo4a. In contrast, light irradiation did not induce an increase in the number of spots in the presence of Dyngo4a although the colocalization of Arrestin<sub>CRY</sub> with ADRB2<sub>CIB</sub> was induced. Considering these results, we concluded that the endocytosis of ADRB2<sub>CIB</sub> was triggered by light-induced interaction of  $\beta$ -arrestin with ADRB2, and the observed ADRB2<sub>CIB</sub> fluorescent spots were ADRB2<sub>CIB</sub>-containing vesicles produced by clathrin-mediated endocytosis.

We further investigated the time dependency of the light-induced endocytosis of ADRB2<sub>CIB</sub>. After HEK293<sub>opt</sub> cells were stimulated with blue light for different durations, the amount of ADRB2<sub>CIB</sub> on the cell surface was quantified using an ELISA<sup>23</sup> (Supplementary Fig. 3a). The amount of ADRB2<sub>CIB</sub> on the cell surface decreased with increasing irradiation time. We also examined the light intensity dependency of endocytosis (Supplementary Fig. 3b). Endocytosis was promoted by increased light intensity and plateaued at 3 mW/cm<sup>2</sup>. The amount of ADRB2<sub>CIB</sub> endocytosed by 3 mW/cm<sup>2</sup> light was more than that induced by 0.01  $\mu$ M ISO and less than that induced by 0.1 and 1.0  $\mu$ M ISO. These results demonstrate that the endocytosis of ADRB2<sub>CIB</sub> can be controlled by modulating light intensity and irradiation time.

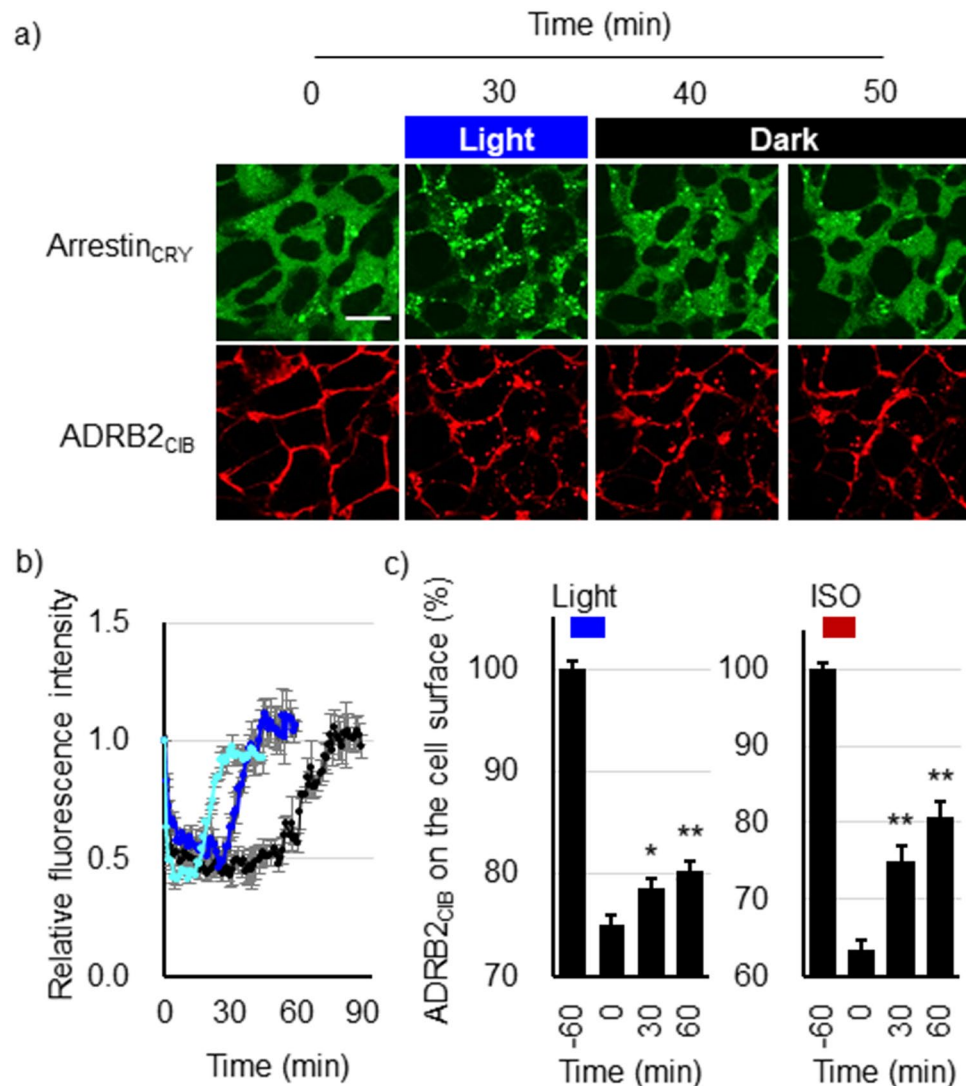


**Figure 3.** Induction of the recycling pathway in the dark after light irradiation. **(a)** Images of Arrestin<sub>CRY</sub> and ADRB2<sub>CIB</sub> fluorescence in HEK293<sub>opt</sub> cells stimulated with blue light for 30 min and then incubated for 10 and 20 min (total of 40 and 50 min observation, respectively) without blue light irradiation. Red, ADRB2<sub>CIB</sub>; green, Arrestin<sub>CRY</sub>. Scale bar, 20  $\mu$ m. **(b)** Time courses of the fluorescence intensity of cytosolic Arrestin<sub>CRY</sub> in each cell. The cells were stimulated with blue light for 15 min (pale blue), 30 min (deep blue), and 60 min (black) and then incubated in the dark. Each time course was normalized to the fluorescence intensity at 0 min. Bars: mean  $\pm$  s.e.m (n = 9 from three individual experiments). **(c)** Recovery of ADRB2<sub>CIB</sub> on the cell surface after stopping irradiation. HEK293<sub>opt</sub> cells were stimulated with blue light (left) or 1.0  $\mu$ M isoproterenol (right) for 60 min. The cells were then incubated at 37  $^{\circ}$ C in the dark for the indicated times. The amount of ADRB2<sub>CIB</sub> on the cell surface was quantified using an ELISA. Bars: mean  $\pm$  s.e.m (n = 12 from three individual experiments). The statistical analysis was performed with Bonferroni post-hoc test (0 min v.s. 30 or 60 min) \**P* values < 0.05 (*P* = 0.024), \*\**P* values < 0.01 (Light; *P* =  $1.9 \times 10^{-3}$ , ISO; *P* =  $8.2 \times 10^{-5}$  (30 min),  $6.6 \times 10^{-7}$  (60 min)).

**Localization of ADRB2<sub>CIB</sub> after Light-Induced Endocytosis.** Most GPCRs are transported to an endocytic pathway after internalization. To confirm that ADRB2<sub>CIB</sub> is transported to endosomes after light-induced endocytosis, we immunostained early and late endosomes using antibodies specific to endosome marker proteins Rab5 and Rab7, respectively (Supplementary Fig. 4a,b). The internalized ADRB2<sub>CIB</sub> was partially localized in Rab5- or Rab7-positive vesicles after 30 min of irradiation. The residual ADRB2<sub>CIB</sub> did not colocalize with the endosomes, indicative of sorting to other endosomes or lysosomes. Based on these results, we concluded that part of the ADRB2<sub>CIB</sub> is transported to endosomes after light-induced endocytosis.

**Induction of the Recycling of ADRB2<sub>CIB</sub> in Dark Conditions.** To show the reversibility of the light-induced interaction between ADRB2<sub>CIB</sub> and Arrestin<sub>CRY</sub>, we irradiated the HEK293<sub>opt</sub> cells with blue light for 30 min and then incubated them in the dark. After Arrestin<sub>CRY</sub> colocalized with ADRB2<sub>CIB</sub>, Arrestin<sub>CRY</sub> redistributed uniformly in the cytosol under dark conditions (Fig. 3a). The fluorescence intensity of Arrestin<sub>CRY</sub> in the



cytosol decreased 1 min after irradiation was started and then recovered to the basal level 10 min after irradiation ceased (Fig. 3b). The colocalization coefficient of Arrestin<sub>CRY</sub> with ADRB2<sub>CIB</sub> decreased after stopping irradiation (Supplementary Fig. 5). The results confirm that Arrestin<sub>CRY</sub> dissociated from ADRB2<sub>CIB</sub> in the dark.

To demonstrate the recycling of ADRB2<sub>CIB</sub> to the cell surface after the dissociation of Arrestin<sub>CRY</sub>, we quantified the amount of ADRB2<sub>CIB</sub> on the cell surface using an ELISA after stopping irradiation. The HEK293<sub>opt</sub> cells were stimulated with blue light for 60 min and then incubated in the dark. The amount of ADRB2<sub>CIB</sub> on the cell surface decreased to 75% after light stimulation and recovered to 80% after 60 min of incubation in the dark (Fig. 3c, left). This result indicates that the recycling of the ADRB2<sub>CIB</sub> was triggered by the dissociation of  $\beta$ -arrestin from ADRB2 in the dark. Furthermore, in HEK293<sub>opt</sub> cells stimulated with ISO, the amount of ADRB2<sub>CIB</sub> on the cell surface recovered from 63 to 77% after ISO was eliminated (Fig. 3c, right). The temporal changes in recycling after light irradiation ceased were similar to those in recycling when ISO was eliminated, demonstrating that temporal control of the dissociation between  $\beta$ -arrestin and ADRB2 is useful for investigating the intracellular dynamics of ADRB2 and regulatory proteins in the recycling pathway.

**Sorting ADRB2<sub>CIB</sub> into the Lysosome Pathway after Prolonged Light Irradiation.** We next investigated the effects of a prolonged interaction of Arrestin<sub>CRY</sub> with ADRB2<sub>CIB</sub> on the sorting of ADRB2<sub>CIB</sub>. HEK293<sub>opt</sub> cells were irradiated with blue light for 120 min. Lysosomes were immunostained with an antibody specific to the lysosome marker protein LAMP1 (Fig. 4a). Sustained light irradiation for 120 min resulted in the disappearance of the ADRB2<sub>CIB</sub> from the cell membrane; instead, ADRB2<sub>CIB</sub> predominantly localized in lysosomes. Furthermore, we examined the colocalization of ADRB2<sub>CIB</sub> with lysosomes (Fig. 4b). The Manders' coefficient increased with increased irradiation time, indicating that the prolonged interaction of Arrestin<sub>CRY</sub> with ADRB2<sub>CIB</sub> drives ADRB2<sub>CIB</sub> to lysosomes. We also examined the ubiquitination of ADRB2<sub>CIB</sub>, which is a crucial signal that sorts GPCRs to lysosomes<sup>24</sup>. Furthermore, ADRB2<sub>CIB</sub> was ubiquitinated to a greater degree when the irradiation time was increased to 120 min (Fig. 4c,d). These results demonstrate that prolonged interaction of  $\beta$ -arrestin with ADRB2, stimulated by blue light, promotes the sorting of ADRB2<sub>CIB</sub> to lysosomes.

**Monitoring a Protein that Regulates ADRB2- $\beta$ -arrestin Complexes.** Some regulatory proteins are recruited to ADRB2- $\beta$ -arrestin complexes; monitoring these regulatory proteins is important to determine their dynamics and functions in trafficking pathways. Mdm2 is a protein that regulates the endocytosis of ADRB2<sup>25</sup>. Although recent studies suggested that Mdm2 has several important roles in the regulation of other membrane receptors, such as the induction of endocytosis of opioid receptors and the activation of a signaling pathway regulated by an IGFR, the dynamics for Mdm2 recruitment to these receptors is unclear<sup>26,27</sup>. To monitor the intracellular dynamics of Mdm2, we established a cell line that stably expresses ADRB2<sub>CIB</sub> and Arrestin<sub>CRY</sub>, but we replaced mCherry with a CLIP tag (HEK293<sub>optCLIP</sub>). HEK293<sub>optCLIP</sub> cells were transfected with cDNA coding mCherry-fused Mdm2 and were then stimulated with blue light under a confocal microscope (Fig. 5a). Before stimulation, most Mdm2 localized on the nucleus, and the residual Mdm2 distributed throughout the cytosol. Several fluorescent spots of Mdm2 were observed in the cytosol after 15 min of light irradiation, and they colocalized with the ADRB2<sub>CIB</sub>-containing vesicles. This result suggests that the cytosolic Mdm2 is recruited to the light-induced ADRB2- $\beta$ -arrestin complexes. The colocalization of Mdm2 with ADRB2<sub>CIB</sub>-containing vesicles was sustained during continuous irradiation (Fig. 5a upper, Movie S2a). In contrast, the Mdm2 dissociated from ADRB2<sub>CIB</sub> 10 min after irradiation ceased (Fig. 5a lower, Movie S2b). We counted the number of Mdm2-recruiting vesicles in the cytosol (Fig. 5b). The number of Mdm2-recruiting vesicles increased with increasing irradiation time but decreased with increasing incubation in the dark. These results indicate that the interaction of  $\beta$ -arrestin with ADRB2 promotes the recruitment of Mdm2 to the ADRB2- $\beta$ -arrestin complex and that the interaction of Mdm2 with the ADRB2<sub>CIB</sub> complex continues until Arrestin<sub>CRY</sub> dissociates from ADRB2<sub>CIB</sub>.

**Examination of the Ability of Arrestin<sub>CRY</sub> to Desensitize ISO-activated ADRB2<sub>CIB</sub>.** Desensitization of ligand-activated GPCRs is one of the important functions of  $\beta$ -arrestin. To examine whether light-induced recruitment of Arrestin<sub>CRY</sub> desensitizes the ISO-activated ADRB2<sub>CIB</sub>, we investigated cAMP production after ISO stimulation under blue light irradiation using cAMP biosensor (Supplementary Fig. 6). The light irradiation did not affect luminescence intensity changes, suggesting that light-induced recruitment of Arrestin<sub>CRY</sub> does not promote desensitization of ADRB2<sub>CIB</sub>.

**Investigation of ADRB2<sub>CIB</sub> Activity during Light Stimulation.** To confirm the activity state of ADRB2<sub>CIB</sub> during the light stimulation, HEK293<sub>opt</sub> cells were transfected with cDNA coding a GFP-fused nanobody (Nb80), which binds specifically to the active state of ADRB2 interacting to G proteins<sup>28</sup>. The cells were stimulated with light or isoproterenol for 30 min under a confocal microscope. The GFP-Nb80 colocalized with ADRB2<sub>CIB</sub>-containing endosomes after ISO stimulation, indicating that the ADRB2<sub>CIB</sub> has an ability to activate the downstream signaling upon ISO stimulation (Supplementary Fig. 7a). In contrast, the colocalization of GFP-Nb80 with ADRB2<sub>CIB</sub> was not observed after light stimulation. To demonstrate the results quantitatively, we quantified the number of spots containing GFP-Nb80 and the colocalization of GFP-Nb80 with ADRB2<sub>CIB</sub>. The spots containing GFP-Nb80 were not observed 30 min after light irradiation, although ISO stimulation induced increases in the number of spots (Supplementary Fig. 7b). The Manders' colocalization coefficient did not change after light stimulation, but increased after ISO stimulation (Supplementary Fig. 7c). These results suggest that endocytosed ADRB2<sub>CIB</sub> by light stimulation does not form the active state required for G protein signaling.

**Investigating the Ability of Arrestin<sub>CRY</sub> to Induce Phosphorylation of ERK1/2.**  $\beta$ -Arrestin, after interacting with ADRB2, functions as a scaffold for the activation of MAPK signaling<sup>29</sup>. Ligand stimulation induces phosphorylation of ADRB2 via G protein-coupled receptor kinases. Phosphorylation of ADRB2 increases the affinity of ADRB2 for  $\beta$ -arrestin and changes the conformation of  $\beta$ -arrestin to form a complex with signaling molecules

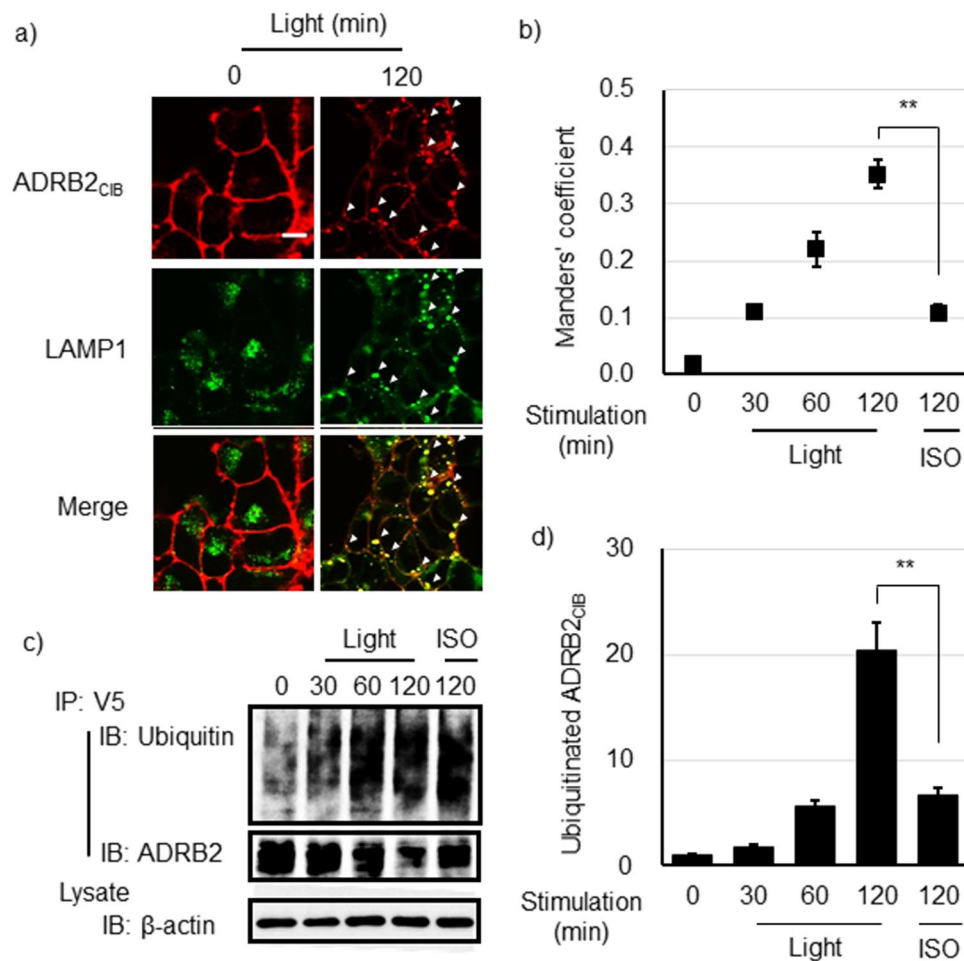


**Figure 4.** Lysosome sorting of ADRB2<sub>CIB</sub> after prolonged irradiation. **(a)** Images of ADRB2<sub>CIB</sub> and lysosome marker LAMP1 fluorescence in HEK293<sub>opt</sub> cells before and after blue light irradiation for 120 min. The white arrowheads indicate the colocalization of ADRB2<sub>CIB</sub> and LAMP1. Red, ADRB2<sub>CIB</sub>; green, LAMP1. Bar, 20 μm. **(b)** Temporal changes in the colocalization of ADRB2<sub>CIB</sub> with lysosomes in HEK293<sub>opt</sub> cells stimulated with blue light for the indicated time or with ISO for 120 min. Data are shown as the mean ± s.e.m. (n = 9 from two independent experiments). The statistical analysis was performed unpaired Student's t-test (two-tailed). \*\* $P < 0.01$  ( $P = 2.0 \times 10^{-7}$ ). **(c)** IP-Western blotting analysis for the detection of ubiquitinated ADRB2<sub>CIB</sub>. HEK293<sub>opt</sub> cells were stimulated with blue light for the indicated time or with 1.0 μM ISO for 120 min. ADRB2<sub>CIB</sub> was immunoprecipitated using an anti-V5-tag antibody. Ubiquitin, ADRB2 and β-actin were blotted with antibodies specific to them. **(d)** The quantified temporal changes in ubiquitinated ADRB2<sub>CIB</sub> were calculated as the ratio of ubiquitinated ADRB2<sub>CIB</sub> to total ADRB2<sub>CIB</sub> quantities, which were determined in the Western blot analysis. The ratio values were normalized to their value at 0 min. Bars: mean ± s.e.m. (n = 9 from three independent experiments). The statistical analysis was performed unpaired Student's t-test (two-tailed). \*\* $P < 0.01$  ( $P = 1.1 \times 10^{-4}$ ).

such as MAPK/ERK kinase (MEK) and ERK1/2, which are then phosphorylated through the interaction with β-arrestin<sup>30–32</sup>. To examine whether Arrestin<sub>CRY</sub> induces phosphorylation of ERK1/2 after the light-induced interaction of Arrestin<sub>CRY</sub> with ADRB2<sub>CIB</sub>, HEK293<sub>opt</sub> cells were irradiated with blue light for 60 min. The phosphorylated ERK1/2 level was evaluated with its specific antibody (Supplementary Fig. 8a). ISO stimulation increased the amount of phosphorylated ERK1/2, whereas the phosphorylated ERK1/2 level decreased after light stimulation. To clarify the reason why light stimulation failed to increase the phosphorylated ERK1/2 level, we investigated phosphorylated ADRB2 (Supplementary Fig. 8b). The phosphorylation of ADRB2<sub>CIB</sub> was not detected after light irradiation. Considering that the phosphorylation of ADRB2 triggers a conformational change in β-arrestin<sup>30–32</sup>, we concluded that Arrestin<sub>CRY</sub> does not recruit ERK1/2 or MEK to the Arrestin<sub>CRY</sub>-ADRB2<sub>CIB</sub> complex due to the lack of ADRB2 phosphorylation.

**Applicability of the Light Activation System to Other Membrane Receptors.** To investigate the applicability of the present system to other membrane receptors, we replaced ADRB2 with different GPCRs such as the neurotensin receptor, muscarinic acetylcholine receptor M3, corticotropin releasing-factor receptor, and vasopressin 2 receptor. All the GPCRs that were investigated in this study localized on the cell surface before

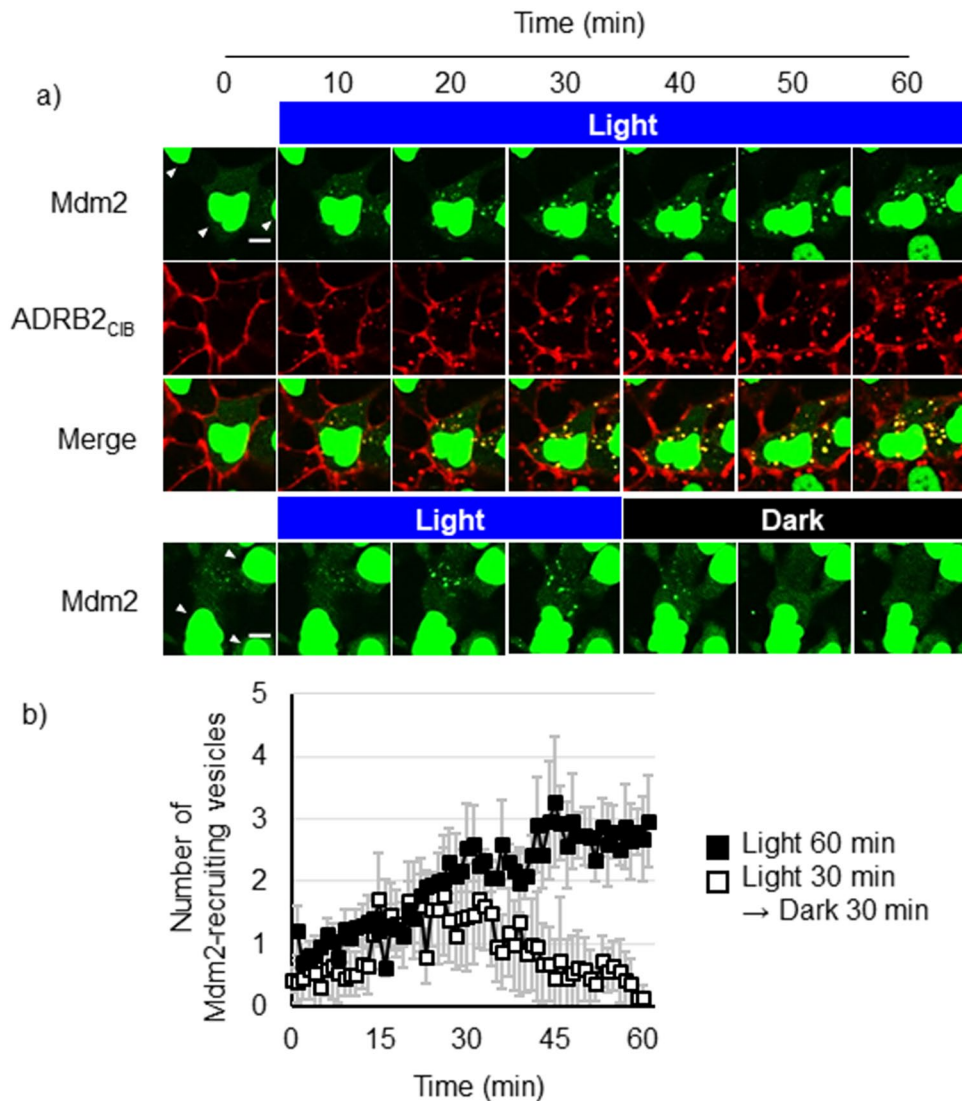


**Figure 5.** Observation of the dynamics of Mdm2 and ADRB2<sub>CIB</sub>. **(a)** Time-lapse images of Mdm2 and ADRB2<sub>CIB</sub> in HEK293<sub>optCLIP</sub> cells. Cells expressing mCherry-fused Mdm2 were stimulated with blue light for 60 min (upper) or for 30 min followed by an additional 30 min in the dark (lower). Red, ADRB2<sub>CIB</sub>; green, mCherry-fused Mdm2. Arrowheads, nuclei. Bar, 10  $\mu$ m. **(b)** Temporal changes in the number of Mdm2-recruiting vesicles per cell. The filled squares show the number of vesicles in cells irradiated for 60 min. The open squares show the number of the vesicles in cells irradiated for 30 min and then incubated in dark for 30 min. Error bars: mean  $\pm$  s.e.m. ( $n = 14$  cells from three individual experiments).

irradiation with blue light. Light stimulation induced translocation of Arrestin<sub>CRY</sub> to the cell surface and endocytosis of the GPCRs (Supplementary Fig. 9a). Furthermore, we applied the method to a non-GPCR receptor, transforming growth factor 3 receptor (TGF3R). TGF3R localized on the cell surface before light stimulation, whereas light stimulation led to the endocytosis of TGF3R, indicating that endocytosis of TGF3R is controllable by the recruitment of  $\beta$ -arrestin to TGF3R. These results demonstrate that the present method is widely applicable to inducing the endocytosis of membrane receptors in living cells. A previous report demonstrated that ERK1/2 phosphorylation was promoted by chemical dimerizer-induced interaction of  $\beta$ -arrestin with V2R<sup>23</sup>, implying different regulations of MAPK activation between ADRB2 and V2R. To examine the difference, we quantified phosphorylated ERK1/2 after light-induced interaction of Arrestin<sub>CRY</sub> with V2R<sub>CIB</sub>. In contrast to the case of ADRB2, the light-induced interaction of  $\beta$ -arrestin with V2R promoted phosphorylation of ERK1/2 30 min after light irradiation (Supplementary Fig. 9b). The results suggest that  $\beta$ -arrestin regulates ERK1/2 phosphorylation in different manners depending on the GPCRs.

## Discussion

We developed an optogenetic method for the analysis of intracellular trafficking of ADRB2 regulated by  $\beta$ -arrestin. We clarified the significance of the interaction of  $\beta$ -arrestin in the intracellular trafficking of ADRB2 using the CRY-CIB system. Endocytosis was promoted by increasing the time that ADRB2 interacts with  $\beta$ -arrestin. The

ADRB2 on the cell surface was recovered after  $\beta$ -arrestin dissociated from ADRB2 in the dark, indicating that the recycling pathway was triggered by the dissociation of  $\beta$ -arrestin from ADRB2. Furthermore, ubiquitination and lysosome sorting were accelerated by prolonged irradiation. These results indicate that the duration of  $\beta$ -arrestin interaction with ADRB2 determines whether ADRB2 takes the lysosomal pathway. In addition, we monitored Mdm2 binding to and dissociating from ADRB2<sub>CIB</sub>-Arrestin<sub>CRY</sub> complexes using light irradiation. Our method monitors the dynamics of ADRB2 and its regulatory proteins in the trafficking pathways. Light-induced manipulation of the interaction of  $\beta$ -arrestin with ADRB2 consequently clarified the regulation of the intracellular trafficking of ADRB2. The present system will be a robust tool for investigating the dynamics of a wide variety of GPCRs and their regulatory proteins in trafficking pathways. Furthermore, we examined other functions of  $\beta$ -arrestin such as desensitization and signaling. Light-induced interaction of  $\beta$ -arrestin with ADRB2 did not promote degradation of cAMP or activation of MAPK. The results indicate that the present method is applicable to controlling the trafficking of ADRB2 without inducing the desensitization or signaling, which is beneficial for investigation of mechanisms of the  $\beta$ -arrestin-mediated trafficking of ADRB2 in living cells and animals.

Controlling the interaction of GPCRs with  $\beta$ -arrestin using the CRY-CIB photoactivation system has several advantages. Previous methods to control the interaction of GPCRs with  $\beta$ -arrestin were based on a chemical approach<sup>23,33</sup>. A pair of chemical dimerizers (FKBP-FRB) were used to control the interaction of  $\beta$ -arrestin with vasopressin receptors or chemokine receptors. However, it is difficult to eliminate rapamycin by simple washing procedures due to its high affinity for FKBP<sup>34</sup>, suggesting that the chemical approach is not suitable for the temporal manipulation of these interactions. The CRY-CIB system is a robust tool to temporally control the reversible interaction of  $\beta$ -arrestin with membrane receptors. The other advantage of the present method is that it can be applied to a wide variety of membrane receptors by connecting CIB to the C-terminus of the target membrane receptor. This approach is useful for the manipulation of orphan GPCRs, whose ligands are undetermined. Recent studies have demonstrated that the trafficking of an orphan GPCR contributes to the pathology of Alzheimer disease<sup>35,36</sup>. However, knowing its specific ligands is required for further analysis of the pathological process. The present method will be useful for the analysis of such orphan GPCRs, without requiring their specific ligands, because the trafficking of GPCRs is controllable by external light. The present method can potentially determine the effects of trafficking a wide variety of membrane receptors on important diseases.

We induced prolonged interactions of  $\beta$ -arrestin with ADRB2 using light irradiation. GPCRs are divided into two classes (class A and class B) depending on their affinity with  $\beta$ -arrestin<sup>14</sup>. ADRB2 is a class A GPCR, members of which interact with  $\beta$ -arrestin for a short period after stimulation by their ligands. We artificially prolonged the interaction of  $\beta$ -arrestin with ADRB2 using light stimulation. The sustained interaction led to greater ubiquitination and lysosome sorting of ADRB2 than stimulation with ISO, suggesting that the duration of the interaction between ADRB2 and  $\beta$ -arrestin determines the amount of ubiquitination and lysosome sorting. In addition, we demonstrated the light-induced endocytosis of 4 different types of GPCRs and a TGF $\beta$ 3R. The light-endocytosed GPCRs are possibly transported in different kinetics because the trafficking is largely influenced by the amino acid residues in the C-terminus<sup>12</sup>. The investigation of the differences provides us valuable information about the significant roles of C-terminus of GPCRs in kinetics regulation of their trafficking without effects of other complicated factors such as ligand affinity to GPCRs and G protein signaling.

We examined the significance of the phosphorylation of ADRB2 in trafficking and signal induction by artificially manipulating the interaction of  $\beta$ -arrestin with ADRB2. The direct manipulation of interactions between specific proteins has been a robust approach for analyzing the significance of protein-protein interactions in complicated intracellular networks<sup>15</sup>. The ligands of ADRB2 activate G proteins via ADRB2 on the cell surface, and the G protein signaling leads to phosphorylation of ADRB2, which increases the affinity of ADRB2 for  $\beta$ -arrestin. The interaction of  $\beta$ -arrestin with ADRB2 on the cell surface induces the endocytosis of ADRB2. We artificially induced the interaction between ADRB2 and  $\beta$ -arrestin via the CRY-CIB system without phosphorylating ADRB2. Light stimulation triggered the endocytosis of ADRB2<sub>CIB</sub>, indicating that phosphorylation of ADRB2 is not necessary to initiate the recruitment of endocytic proteins such as clathrin and Mdm2 to ADRB2- $\beta$ -arrestin complexes. However, the maximum induction level of the endocytosis of ADRB2<sub>CIB</sub> after light stimulation was lower than that induced by 0.1 and 1.0  $\mu$ M ISO. The result implies that phosphorylation of ADRB2 is required for the efficient endocytosis of ADRB2 from the plasma membrane. We also evaluated the induction level of MAPK signaling after light irradiation. The level of phosphorylated ERK1/2 unexpectedly decreased after light irradiation. Although the reason for the phosphorylation decrease after light stimulation is not clear, the result indicates that other factors increase the amount of phosphorylated ERK1/2. For example, phosphorylated ADRB2 facilitates  $\beta$ -arrestin adopting a specific conformation to form an ADRB2- $\beta$ -arrestin-MEK-ERK1/2 complex<sup>30–32</sup>. We speculated that the lack of increase in phosphorylated ERK1/2 after light stimulation was due to the lack of phosphorylated ADRB2. To confirm the conformation of  $\beta$ -arrestin, several FRET- and BRET-based indicators were reported<sup>23,37</sup>. However, these indicators contain bioluminescent, fluorescent proteins or chemical dyes, of which absorption and emission wavelength overlap with absorption wavelength of CRY, suggesting a possibility that the overlap hampers a precise detection of the conformation of  $\beta$ -arrestin. To overcome the issue, use of a FRET indicator with another absorption and emission wavelength such as mKate and iRFP will be needed. Combination of a novel indicators and the present system will provide powerful approaches for investigation of the relevance between conformation of  $\beta$ -arrestin and intracellular trafficking on cell surface and endosomes. In addition, several studies have demonstrated that the rapamycin-induced interaction of  $\beta$ -arrestin with vasopressin receptors or chemokine receptors promotes the phosphorylation of ERK1/2<sup>23,33</sup>. Light-induced interaction of  $\beta$ -arrestin with V2R also activated the phosphorylation of ERK1/2. The result using ADRB2 is completely different from the results of the reports and our result, suggesting that the activation of MAPK signaling depends on the type of GPCR. We consequently suggested that the light-induced interaction of  $\beta$ -arrestin with ADRB2 is not sufficient for the activation of MAPK signaling, which is a significant clue to understanding the mechanisms of activation of  $\beta$ -arrestin-mediated signals.



We developed the photoinducible GPCR- $\beta$ -arrestin interaction systems, and utilized them for investigation of the significant roles of  $\beta$ -arrestin on the endocytosis and intracellular trafficking of GPCRs. In addition, there are other potential applications of the present methods. Previous studies demonstrated importance of GPCR conformations for activation and inactivation of downstream signaling<sup>28</sup>. However, it is not well investigated whether the conformational state of GPCRs influences on their intracellular trafficking. The trafficking of GPCRs in a specific conformation may be possibly investigated using the present system together with antagonists or inverse agonists that induce specific GPCR conformations. This approach will clarify significant roles of conformational states of GPCRs on intracellular trafficking. In addition, a previous study also suggested the possibility of the endocytosis of G proteins with some GPCRs<sup>38</sup>, whereas another study on single molecule imaging reported that G protein-ADRB2 complexes did not colocalize with clathrin-coated pits<sup>39</sup>. Thus, it is not clear whether the interaction of G protein with GPCRs affects their endocytosis. The present system may be applicable to clarify the impact of G proteins on the receptor internalization by comparing the dynamics of endocytosis between ligand-activated GPCRs interacting with G proteins and light-stimulated GPCRs without G proteins. Furthermore, the present method has a potential to control the oligomeric state of the GPCRs. GPCRs form dimers and oligomers upon stimulation of their ligands, which is important for recruitment of their regulatory proteins on cell surface<sup>40</sup>. Based on the fact that the light-activated CRY and CIB forms oligomers<sup>41</sup>, ADRB2<sub>CIB</sub> and Arrestin<sub>CRY</sub> also form oligomers upon light stimulation. Light control of the oligomeric state of ligand-stimulated GPCRs will be a useful approach to investigate the oligomerization of GPCRs affecting their regulatory proteins in living cells.

In conclusion, we developed a novel method that uses the CRY-CIB system to manipulate the interaction between  $\beta$ -arrestin and ADRB2. Temporal manipulation of the interaction between  $\beta$ -arrestin and ADRB2 using this optogenetic system revealed the  $\beta$ -arrestin-mediated regulation of the intracellular trafficking of ADRB2. Endocytosis of ADRB2 was promoted by increased light intensity and irradiation time. The dissociation of  $\beta$ -arrestin from ADRB2 under dark conditions triggered the recycling of the endocytosed ADRB2 to the cell surface, whereas the prolonged interaction of  $\beta$ -arrestin with ADRB2 promoted the sorting of ADRB2 to lysosomes. The duration of the reversible interaction of  $\beta$ -arrestin with ADRB2 therefore determines the intracellular trafficking of ADRB2. In addition, the recruitment of the regulatory protein Mdm2 to ADRB2- $\beta$ -arrestin complexes was driven by light induction of the interaction between  $\beta$ -arrestin and ADRB2. Our method will be effective for investigating the dynamics of GPCRs and their regulatory proteins in trafficking pathways. Furthermore, MAPK signaling was not activated through the light-induced interaction of  $\beta$ -arrestin with ADRB2; this behavior may be due to the light-induced interaction not causing a conformational change in  $\beta$ -arrestin that results in recruitment of MEK and ERK1/2. We consequently showed that the artificial induction of interactions between membrane receptors and their regulatory proteins via an optogenetic tool is a useful approach for investigating the intracellular trafficking of membrane receptors. Light-induced internalization of membrane receptors on cell surfaces and the manipulation of intracellular trafficking will be beneficial to unveiling significant roles of membrane receptors in living tissues and will also be useful for investigating the pathological processes of important diseases.

## Methods and Materials

**Materials and cDNA Construction.** SNAP-Surface Alexa Fluor 647 and anti-SNAP-tag antibodies were obtained from New England Biolabs (USA). ISO and Dyngo4a were purchased from Tokyo Chemical Industry (Japan) and Abcam (USA), respectively. Anti-Rab5, anti-Rab7, anti-LAMP1, anti-ERK1/2 and anti-phosphorylated ERK1/2 antibodies were obtained from Cell Signaling Technology (USA). Anti- $\beta$ 2-adrenergic receptor (ADRB2) and anti-phosphorylated ADRB2 antibodies were purchased from Santa Cruz Biotechnology (USA). The SNAP-Surface Alexa Fluor 647 and Dyngo4a were solved in DMSO. The ISO was solved in H<sub>2</sub>O. The DNA fragments encoding SNAP-tag, ADRB2 and CIB were inserted between *Hind*III and *Xho*I sites in pcDNA3.1/V5-His (B) (Thermo Fisher Scientific, USA). The genes encoding CRY, mCherry and  $\beta$ -arrestin 2 were subcloned between *Bam*HI and *Xba*I sites in pcDNA4/myc-His (B) (Thermo Fisher Scientific).

**Cell Cultivation.** HEK293 cells were cultured in Dulbecco's Modified Eagle Medium (D-MEM, Wako Pure Chemical Industry, Japan) containing 10% fetal bovine serum (FBS, Sigma-Aldrich, USA) and 1% penicillin/streptomycin (Gibco, Thermo Fisher Scientific, USA) under a 5% CO<sub>2</sub> atmosphere at 37 °C. D-MEM supplemented with 10% FBS, 1% penicillin/streptomycin, 400  $\mu$ g/ml G418 (Gibco) and 100  $\mu$ g/ml zeocin (Thermo Fisher Scientific) was used for cultivating HEK293 cells stably expressing fusion proteins (HEK293<sub>opt</sub> and HEK293<sub>optCLIP</sub>).

**Confocal Fluorescence Microscopy.** Cells were cultured on 35-mm glass-bottomed dishes. To label the SNAP-tag, 0.5  $\mu$ M SNAP-Surface Alexa Fluor 647 was added to the medium, and the cells were incubated for 30 min at 37 °C. After the cells were washed three times, the medium was exchanged by 2 ml of phenol red-free D-MEM containing HEPES, pH 7.4 (Wako Pure Chemical Industry). The cells were observed under a confocal microscope (IX-81, FV-1000D, Olympus). The images were acquired every 1 min. CRY activation was performed under a confocal microscope using a 20 mW 440-nm laser at 0.5% output with a scan speed of 2.0  $\mu$ s/pixel. The fluorescence intensity of Arrestin<sub>CRY</sub> was evaluated using the image analysis software FV10-ASW (Olympus). The number of ADRB2<sub>CIB</sub> or Mdm2 fluorescence spots was counted using ImageJ. The diameter to detect the spots was set at 0.5–5  $\mu$ m.

**Immunostaining of Early Endosomes, Late Endosomes and Lysosomes.** HEK293<sub>opt</sub> cells were cultured on 35-mm glass-bottomed dishes. ADRB2<sub>CIB</sub> was labeled with SNAP-Surface Alexa Fluor 647 for 30 min and then washed three times with D-MEM. The cells were cultured in D-MEM and stimulated with blue light at an intensity of 3 mW/cm<sup>2</sup> using an LED device (TH-211  $\times$  200BL, Creating Customer Satisfaction, Japan) for the indicated times. The cells were fixed using 4% formaldehyde and then permeabilized with 0.2% Triton X-100. To

avoid the non-specific adsorption of antibodies, the cells were treated with 0.2% gelatin from cold-water fish skin (Sigma-Aldrich) for 1 h at room temperature. Rab5, Rab7 and LAMP1 were labeled with the corresponding antibodies in PBS(+) overnight at 4 °C. After the cells were washed three times with PBS(+), they were stained with Alexa Fluor 488-conjugated goat anti-Rabbit IgG Secondary Antibody (Thermo Fisher Scientific) for 1 h at room temperature. The cells were washed three times with PBS(+) and then observed under a confocal microscope.

**Calculation of Manders' Colocalization Coefficient.** The extent of the colocalization of ADRB2<sub>CIB</sub> with lysosomes was estimated using Manders' colocalization coefficient.

$$\text{Manders' colocalization coefficient} = \frac{\sum_j FI_{j\text{coloc}}}{\sum_i FI_i}$$

where  $FI_i$  is the fluorescence intensity of Alexa Fluor 647 molecules attached to ADRB2<sub>CIB</sub> in the pixel  $i$ , and  $FI_{j\text{coloc}} = 0$  if the fluorescence intensity of Alexa 488, which is attached to LAMP1, in the pixel  $j$  is lower than a particular threshold, and  $FI_{j\text{coloc}} = FI_j$  if the fluorescence intensity of Alexa 488 in pixel  $j$  is equal to or larger than the threshold. The coefficient was calculated using the JACoP plug-in for ImageJ after applying a threshold of fluorescent intensity to each time-lapse image<sup>42</sup>. The thresholds were automatically determined based on the JACoP program.

**Quantification of ADRB2<sub>CIB</sub> on the Cell Surface Using the ELISA Assay.** HEK293<sub>opt</sub> cells in 4-well plates were treated with 1.0 μM ISO or irradiated with blue light at 3 mW/cm<sup>2</sup> for the indicated time. After the cells were fixed with 4% formaldehyde, they were treated with gelatin from cold-water fish skin for blocking. SNAP-tag moieties on the cell surface were labeled with an anti-SNAP-tag antibody for 60 min at room temperature. After the cells were washed twice with PBS(+), ECL anti-rabbit antibody linked to HRP was added to each well. The cells were incubated for 60 min at room temperature and then washed three times with PBS(+). After the addition of 350 μl of TMB solution (Thermo Fisher Scientific) and 30 min of incubation, 350 μl of 2 M sulfuric acid was added to each well. The OD<sub>450</sub> value of 100 μl of solution was measured using a microplate reader (Bio-Rad, USA). The amount of ADRB2<sub>CIB</sub> on the cell surface was defined by  $(\text{OD} - \text{OD}^{\text{mock}})/(\text{OD}^{\text{basal}} - \text{OD}^{\text{mock}}) \times 100$ , where OD<sup>mock</sup> and OD<sup>basal</sup> correspond to the OD of non-stimulated HEK293 cells and the OD from non-stimulated HEK293<sub>opt</sub>, respectively. To promote recycling of ADRB2<sub>CIB</sub> in ISO-treated cells, cells were washed three times with 500 μl of acidic buffer (150 mM NaCl and 5 mM acetic acid) and then twice with 500 μl of PBS(+) to eliminate ISO.

**Detection of Ubiquitinated ADRB2<sub>CIB</sub> Using Immunoprecipitation.** HEK293<sub>opt</sub> cells that had been cultured on a 4-well plate were stimulated with 3 mW/cm<sup>2</sup> blue light using the LED device or 1.0 μM ISO for the indicated time. The cells were harvested using 200 μl of lysis buffer (50 mM HEPES (pH 7.5), 0.5% NP-40, 250 mM NaCl, 2 mM EDTA, 10% glycerol, 1 mM sodium orthovanadate, 1 mM sodium fluoride, 1 mM phenylmethylsulfonyl fluoride, 10 mg/ml leupeptin and MG-132 proteasome inhibitor). Anti-V5 antibody (Life Technologies) was added to each lysate, which was then gently shaken at 4 °C for 1 h. After protein G Sepharose (GE Healthcare, USA) was added, the lysate was shaken at 4 °C for 1 h. The precipitate was washed three times with 1 ml of lysis buffer and dissolved in 100 μl of sample buffer (125 mM Tris, pH 6.8, 10% glycerol, 4% SDS, 0.006% bromophenol blue and 10% mercaptoethanol). The samples were heated at 65 °C for 10 min and then subjected to SDS-PAGE using 10% acrylamide gels. The proteins were transferred onto nitrocellulose membranes (Bio-Rad, USA). To block the non-specific binding of antibodies, the membrane was treated with 1% skim milk in Tris-buffered saline for 1 h. ADRB2 and ubiquitin were blotted using their corresponding antibodies. The blotted bands were detected using an image analyzer (ImageQuant LAS-4000, GE Healthcare), and the intensity of each band was measured with an ImageQuant TL software.

**Statistical Analysis.** Statistical significance was determined using unpaired Student's t-tests (two-tailed) and Bonferroni post-hoc test. Differences with  $P$  values < 0.05 were considered statistically significant.

## References

- Zerial, M. & McBride, H. Rab proteins as membrane organizers. *Nat. Rev. Mol. Cell Biol.* **2**, 107–117 (2001).
- Hutagalung, A. H. & Novick, P. J. Role of Rab GTPases in Membrane Traffic and Cell Physiology. *Physiol. Rev.* **91**, 119–149 (2011).
- Sanders, C. R. & Myers, J. K. Disease-related misassembly of membrane proteins. *Annu. Rev. Biophys. Biomol. Struct.* **33**, 25–51 (2004).
- Amara, J. F. & Cheng, S. H. & Smith, a. E. Intracellular protein trafficking defects in human disease. *Trends Cell Biol.* **2**, 145–149 (1992).
- Marchese, A., Paing, M. M., Temple, B. R. S. & Trejo, J. G Protein-Coupled Receptor Sorting to Endosomes and Lysosomes. *Annu. Rev. Pharmacol. Toxicol.* **48**, 601–629 (2008).
- Hanyaloglu, A. C. & von Zastrow, M. Regulation of GPCRs by Endocytic Membrane Trafficking and Its Potential Implications. *Annu. Rev. Pharmacol. Toxicol.* **48**, 537–568 (2008).
- Jean-Alphonse, F. & Hanyaloglu, A. C. Regulation of GPCR signal networks via membrane trafficking. *Mol. Cell. Endocrinol.* **331**, 205–214 (2011).
- Moore, C. A. C., Milano, S. K. & Benovic, J. L. Regulation of Receptor Trafficking by GRKs and Arrestins. *Annu. Rev. Physiol.* **69**, 451–482 (2007).
- Chen, W. *et al.* β-arrestin 2 mediates endocytosis of type III TGF-β receptor and down-regulation of its signaling. *Science* **301**, 1394–1397 (2003).
- Lin, F. T., Daaka, Y. & Lefkowitz, R. J. β-arrestins regulate mitogenic signaling and clathrin-mediated endocytosis of the insulin-like growth factor I receptor. *J. Biol. Chem.* **273**, 31640–31643 (1998).
- Zhang, J. *et al.* Cellular Trafficking of G Protein-coupled Receptor/β-Arrestin Endocytic Complexes. *J. Biol. Chem.* **274**, 10999–11006 (1999).
- Oakley, R. H., Laporte, S. A., Holt, J. A., Barak, L. S. & Caron, M. G. Association of β-arrestin with G protein-coupled receptors during clathrin-mediated endocytosis dictates the profile of receptor resensitization. *J. Biol. Chem.* **274**, 32248–32257 (1999).

13. Shenoy, S. K. & Lefkowitz, R. J. Trafficking Patterns of  $\beta$ -Arrestin and G Protein-coupled Receptors Determined by the Kinetics of  $\beta$ -Arrestin Deubiquitination. *J. Biol. Chem.* **278**, 14498–14506 (2003).
14. Lefkowitz, R. J. & Shenoy, S. K. Transduction of Receptor Signals. *Science* **308**, 512–518 (2005).
15. Tischer, D. & Weiner, O. D. Illuminating cell signalling with optogenetic tools. *Nat. Rev. Mol. Cell Biol.* **15**, 551–558 (2014).
16. Zhang, K. & Cui, B. Optogenetic control of intracellular signaling pathways. *Trends Biotechnol.* **33**, 92–100 (2015).
17. Weitzman, M. & Hahn, K. M. Optogenetic approaches to cell migration and beyond. *Curr. Opin. Cell Biol.* **30**, 112–120 (2014).
18. Kennedy, M. J. *et al.* Rapid blue-light-mediated induction of protein interactions in living cells. *Nat. Methods* **7**, 973–975 (2010).
19. Nguyen, M. K. *et al.* Optogenetic oligomerization of Rab GTPases regulates intracellular membrane trafficking. *Nat. Chem. Biol.* **12**, 431–436 (2016).
20. Koch, W. J., Lefkowitz, R. J. & Rockman, H. A. Functional consequences of altering myocardial adrenergic receptor signaling. *Annu. Rev. Physiol.* **62**, 237–60 (2000).
21. Johnson, M. Molecular mechanisms of  $\beta$ 2-adrenergic receptor function, response, and regulation. *J. Allergy Clin. Immunol.* **117**, 18–24 (2006).
22. Zhang, J., Barak, L. S., Winkler, K. E., Caron, M. G. & Ferguson, S. S. A central role for  $\beta$ -arrestins and clathrin-coated vesicle-mediated endocytosis in  $\beta$ 2-adrenergic receptor resensitization. *J. Biol. Chem.* **272**, 27005–27014 (1997).
23. Terrillon, S. & Bouvier, M. Receptor activity-independent recruitment of  $\beta$ arrestin2 reveals specific signalling modes. *EMBO J.* **23**, 3950–3961 (2004).
24. Shenoy, S. K., McDonald, P. H., Kohout, T. A. & Lefkowitz, R. J. Regulation of receptor fate by ubiquitination of activated  $\beta$ 2-adrenergic receptor and  $\beta$ -arrestin. *Science* **294**, 1307–1313 (2001).
25. Shenoy, S. K. *et al.*  $\beta$ -Arrestin-dependent signaling and trafficking of 7-transmembrane receptors is reciprocally regulated by the deubiquitinase USP33 and the E3 ligase Mdm2. *Proc. Natl Acad. Sci. USA* **106**, 3–8 (2009).
26. Wang, P. *et al.*  $\beta$ -Arrestin 2 Functions as a G-Protein-coupled Receptor-activated Regulator of Oncoprotein Mdm2. *J. Biol. Chem.* **278**, 6363–6370 (2003).
27. Girnita, L. *et al.*  $\beta$ -arrestin is crucial for ubiquitination and down-regulation of the insulin-like growth Factor-1 receptor by acting as adaptor for the MDM2 E3 ligase. *J. Biol. Chem.* **280**, 24412–24419 (2005).
28. Nygaard, R. *et al.* The dynamic process of  $\beta$ 2-adrenergic receptor activation. *Cell* **152**, 532–542 (2013).
29. Nobles, K. N. *et al.* Distinct Phosphorylation Sites on the  $\beta$ 2-Adrenergic Receptor Establish a Barcode That Encodes Differential Functions of  $\beta$ -Arrestin. *Sci. Signal.* **185**, 1–10 (2012).
30. Charest, P. G., Terrillon, S. & Bouvier, M. Monitoring agonist-promoted conformational changes of  $\beta$ -arrestin in living cells by intramolecular BRET. *EMBO Rep.* **6**, 334–340 (2005).
31. Lee, M. *et al.* The conformational signature of arrestin3 predicts its trafficking and signalling functions. *Nature* **531**, 665–668 (2016).
32. Nuber, S. *et al.*  $\beta$ -Arrestin biosensors reveal a rapid, receptor-dependent activation/deactivation cycle. *Nature* **531**, 661–664 (2016).
33. Liebick, M., Henze, S., Vogt, V. & Oppermann, M. Functional consequences of chemically-induced  $\beta$ -arrestin binding to chemokine receptors CXCR4 and CCR5 in the absence of ligand stimulation. *Cell. Signal.* **38**, 201–211 (2017).
34. Lin, Y. *et al.* Rapidly Reversible Manipulation of Molecular Activity with Dual Chemical Dimerizers. *Angew. Chem. Int. Edn Engl.* **52**, 6450–6454 (2013).
35. Thathiah, A. *et al.* The orphan G protein-coupled receptor 3 modulates amyloid- $\beta$  peptide generation in neurons. *Science* **323**, 946–951 (2009).
36. Thathiah, A. *et al.*  $\beta$ -arrestin 2 regulates A $\beta$  generation and  $\gamma$ -secretase activity in Alzheimer's disease. *Nat. Med.* **19**, 43–9 (2013).
37. Lee, M. *et al.* The conformational signature of  $\beta$ -arrestin2 predicts its trafficking and signalling functions. *Nature* **531**, 665–668 (2016).
38. Ferrandon, S. *et al.* Sustained cyclic AMP production by parathyroid hormone receptor endocytosis. *Nature Chem. Biol.* **5**, 734–742 (2009).
39. Sungkaworn, T. *et al.* Single-molecule imaging reveals receptor–G protein interactions at cell surface hot spots. *Nature* **550**, 543–547 (2017).
40. George, S. R., O'Dowd, B. F. & Lee, S. P. G-protein-coupled receptor oligomerization and its potential for drug discovery. *Nat. Rev. Drug Discov.* **1**, 808–820 (2002).
41. Che, D. L., Duan, L., Zhang, K. & Cui, B. The dual characteristics of light-induced cryptochrome 2, homo-oligomerization and heterodimerization, for optogenetic manipulation in mammalian cells. *ACS Synth. Biol.* **4**, 1124–1135 (2015).
42. Bolte, S. & Cordelières, F. P. A guided tour into subcellular colocalization analysis in light microscopy. *J. Microsc.* **224**, 213–232 (2006).

## Acknowledgements

This work was supported by the Japan Society for the Promotion of Science (JSPS) and the Ministry of Education, Culture, Sports, Science, and Technology (MEXT) of Japan (Grants-in-Aid for Scientific Research S 26220805, and on Innovative Areas 26620128 to T.O., and for Encouragement of Young Scientists A 25708025 to H.Y.). This work was also supported in part by grants from the Asahi Glass Foundation to T.O.

## Author Contributions

O.T., H.Y., and T.O. conceived the project. O.T. and H.Y. performed the experiments and analysis. O.T., H.Y., and T.O. wrote the manuscript.

## Additional Information

**Supplementary information** accompanies this paper at <https://doi.org/10.1038/s41598-017-19130-y>.

**Competing Interests:** The authors declare that they have no competing interests.

**Publisher's note:** Springer Nature remains neutral with regard to jurisdictional claims in published maps and institutional affiliations.



**Open Access** This article is licensed under a Creative Commons Attribution 4.0 International License, which permits use, sharing, adaptation, distribution and reproduction in any medium or format, as long as you give appropriate credit to the original author(s) and the source, provide a link to the Creative Commons license, and indicate if changes were made. The images or other third party material in this article are included in the article's Creative Commons license, unless indicated otherwise in a credit line to the material. If material is not included in the article's Creative Commons license and your intended use is not permitted by statutory regulation or exceeds the permitted use, you will need to obtain permission directly from the copyright holder. To view a copy of this license, visit <http://creativecommons.org/licenses/by/4.0/>.

© The Author(s) 2018